Photosynthetic Light Reactions at the Gold Interface

Kamran, M.

CHAPTER 3

Photosynthetic protein complexes as bio-photovoltaic building blocks with a high internal quantum efficiency

Abstract

Photosynthetic compounds have been a paradigm for biosolar cells and biosensors and for application in photovoltaic and photocatalytic devices. However, the interconnection of proteins and protein complexes with electrodes, in terms of electronic contact, structure, alignment and orientation, remains a challenge. Here we report on a deposition method that relies on the self organizing properties of these biological protein complexes to produce a densely packed and uniformly oriented monolayer by using Langmuir-Blodgett technology. The monolayer was deposited onto a gold electrode with defined orientation and produces the highest light induced photocurrents per protein complex to date, 45 $\mu A/cm^2$ (with illumination power of 23 mW/cm^2 at 880 nm) under ambient conditions. Our work shows for the first time that a significant portion of the intrinsic quantum efficiency of primary photosynthesis can be retained in a functional device outside the biological cell, leading to an internal quantum efficiency of 32% for light-induced electron transfer from the electrode to the photosynthetic protein complex.

3.1- Introduction

The design characteristics of photosynthesis are paradigm in solar cell research primarily because of the high, near unity quantum efficiency of the light driven steps in this process.[1] The primary photo-conversion reactions involve light absorption, energy transfer and charge transfer. The process relies on the interplay between various types of light-harvesting protein complexes, structurally well-defined polymers with embedded light-absorbing chromophores held in exact geometries. Besides mimicking individual aspects of photosynthesis there is a growing interest for the direct application of the protein complexes in biosolar cells and biosensors.[2-12] However, the interconnection of proteins and protein complexes with electrodes, in terms of electronic contact, structure, alignment and orientation, remains a challenge. Several immobilization techniques have been examined in the past, which mostly involved bio-films formed by self-assembly on the surface of electrodes by incubation in a solution of photosynthetic complexes.[13-19] Even though photosynthetic proteins readily adsorb on the electrode, these techniques often produce monolayers with a non-uniform protein orientation. In order to control the orientation of the complexes on the electrodes, much research has been aimed at the development of genetically engineered complexes that bind specifically to an electrode that has been pre-modified with a suitable monolayer of linker molecules.[5,20-26] A drawback of this method is the decrease in electron transfer (ET) efficiency due to the increased tunneling distance introduced by the thickness of the monolayer of linker molecules. A variety of photosynthetic proteins have been explored within the context of bio-hybrid devices, with emphasis on photosystem I (PSI), photosystem II (PSII), and reaction center (RC) complexes from different photosynthetic organisms.[4-6,9,10,12,13,18-20,24,27-36] As far as we know the quantum efficiency of any photosynthesis based biohybrid device reported has always been extremely low, with one moderate exception of 12% reported by Das et al. albeit upon illumination by monochromatic laser light of $10W/cm^2$, the equivalent of more than 100 suns.[5]

Here we report on the Langmuir-Blodgett method that relies on the self-organizing properties of photosynthetic protein complexes to produce a uniformly oriented, densely packed monolayer of photosynthetic proteins. This method stands out by its simplicity, and by depositing Langmuir-Blodgett films directly onto a bare gold

electrode we produce record photocurrents with an internal quantum efficiency of 32%, under illumination by a light emitting diode with intensity of 23 mW/cm^2.

The Langmuir-Blodgett (LB) technique (see Figure 1) has been widely used for the deposition of mono- or multilayers of amphiphilic molecules on to solid substrates.[37-47] This method relies on the fact that when spread on a water surface, amphiphilic molecules take on a particular orientation with their hydrophilic side facing the water and their hydrophobic side facing upward (see Figure 1). The end result is a highly oriented monolayer of the sample at the air-water interface. This monolayer can then be deposited onto a particular substrate by vertically dipping the substrate into the water sub-phase. By reversing the dipping procedure, from the water phase into air, the orientation of the protein complexes is expected to be reversed as well. In this study, we employ isolated bacterial reaction center-light harvesting 1 (RC-LH1) complexes from the photosynthetic purple bacterium *Rhodopseudomonas (Rps.) acidophila*. The cylindrical wall of the RC-LH1 complex is strongly hydrophobic which explains its propensity for self-assembly in 2D arrays and its affinity for lipid bylayers. The two end-surfaces are more hydrophilic, but the difference between them may be sufficient to induce a preferred orientation upon the assembly of a LB layer. In the case of *Rb. sphaeroides*, for example, RCs in LB films are oriented with their H-subunit towards the water phase.[48] RCs from *Rps. viridis*, however, have the opposite

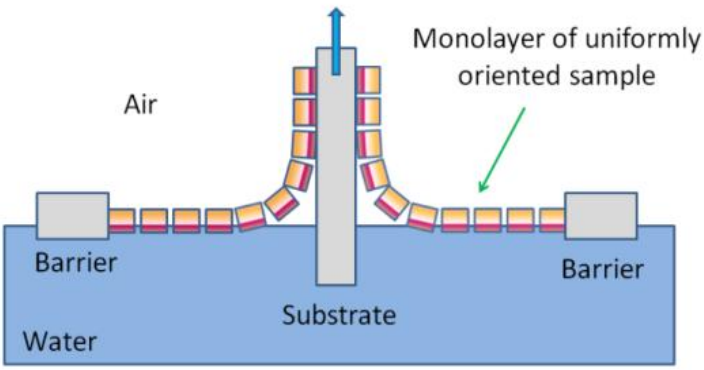

Figure 1. Schematic representation of the Langmuir-Blodgett deposition method. A sample containing amphiphilic molecules form a uniformly oriented monolayer on the water-air interface, with its hydrophilic side (purple) facing the water and its hydrophobic side (yellow) pointing upwards. The sample retains its orientation as it is being deposited on the substrate.

orientation because of the more hydrophilic cytochrome subunit at the periplasmic side of the complex.[48]

The LH1 complex is a cylindrically shaped protein complex with a diameter of approximately 11 nm that contains 48 light absorbing pigments, including 32 bacteriochlorophylls and 16 carotenoid molecules. Light is absorbed by these pigments and excitations are transferred among the complexes until they are trapped by the reaction center which is surrounded by the LH1 proteins. The reaction center consists of several pigments and once an excitation is trapped, charge is transferred along a well-defined branch of redox-active cofactors in the RC, *i.e.* from a special bacteriochlorophyll *a* dimer to a pair of ubiquinone acceptors (Q_A and Q_B) via an intermediary bacteriochlorophyll *a* and a bacteriopheophytin molecule.

In nature this RC-LH1 complex is embedded in a lipid bilayer in a uniform orientation often mixed with additional light harvesting 2 (LH2) complexes. In several purple bacterial, photosynthetic species domains are formed of clusters of RC-LH1 complexes with varying size and order. likely assisted by the hydrophobic character of the outer walls of the cylindrical protein structure. This particular feature also drives the formation of RC-LH1 complexes to orient in two dimensional arrays on the water-air interface of a Langmuir–Blodgett (LB) trough. In order to make surface-adhered protein complexes viable for technological applications, some basic issues need to be addressed. Two of the main concerns are the preservation of the functional integrity of the proteins once they are adhered on conducting surfaces, and the efficiency of electron transfer between the protein and the electrode.

3.2 Materials and Methods

Langmuir Blodgett film deposition

The LB films were deposited on a gold sputtered glass slide by vertically dipping it into the sub-phase (forward dipping) or pulling it out (reverse dipping). The sub-phase of the LB trough consisted of milli-Q water. Before dipping, a solution of isolated RC-LH1 complexes was spread over the water surface and compressed to a surface pressure of 50 mN/m. In order to avoid structural deformation and achieve higher surface coverage, the surface pressure was kept constant at 50

mN/m during the LB deposition.[42] In forward dipping mode, the gold coated glass slide was vertically dipped with a velocity of 1 mm/min and then removed at the highest available speed in order to avoid any deposition during the extraction. In reverse dipping the gold coated slide was dipped into the sub-phase before spreading the RC-LH1 complexes on the water surface. After compression of the LB-film the slide was pulled out slowly at a constant surface pressure of 50 mN/m to deposit the complexes with their hydrophilic side facing the electrode.

3.2.1 Photocurrent measurements

After the LB deposition step, the slide was incorporated into a measuring cell containing 2 ml of Tris buffer solution (pH 8). Light induced current measure-

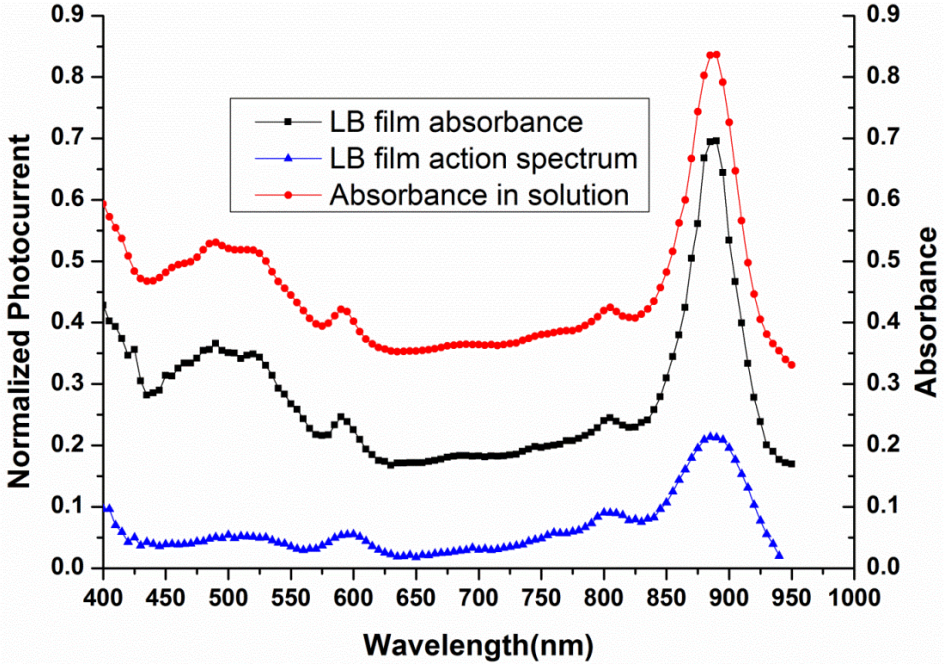

Figure 2. Action spectrum (blue triangles) and absorption spectra (black squares, forward dipped) of isolated RC-LH1 complexes deposited by the Langmuir-Blogdett method on a bare gold electrode. The action spectrum is obtained by measuring the photocurrent as a function of wavelengths, and is normalized for the intensity of light illumination. Absorption of isolated RC-LH1 complexes in buffer solution (red circles, Tris-HCl pH8) is shown for comparison. The absorption spectra are vertically displaced for better viewing. The vertical right-hand scale applies to the absorption spectrum; the LB-absorption spectrum is stretched vertically by a factor of 70.

ments were carried out using a potentiostat employing a conventional three-electrode setup, with the gold layer acting as the working electrode, a saturated calomel electrode as reference and a platinum wire serving as the counter electrode. The sample was illuminated from below, through the gold layer which was 12 nm thick with an optical transmission of 51 % at 880 nm, see Figure S1 in Supplementary Information (SI-3). The light source was a light emitting diode (LED) centered at λ = 880 nm, with a bandwidth of 50 nm, providing a light intensity of 23 mW/cm^2 at the surface of the working electrode of the electrochemical cell.

For measuring the action spectrum the excitation wavelength was scanned by passing white light (from a tungsten/halogen lamp) through a monochromator with a bandwidth of 40 nm. In this case, the light intensity at the surface of the electrode was 2 mW/cm^2 at λ = 880 nm. More details of experimental conditions and procedures are available in Supporting Information. The Tris-buffered electrolyte contained ubiquinone-0 (Q-0) and horse heart cytochrome (cyt\) *c* as redox mediators which are responsible for electron transport from the Q_B site to the counter electrode and to assist the reduction of the special pair of the RC at the gold electrode.

3.3 Results and discussion

First of all we note that the absorption spectrum of the LB-deposited layer on the gold electrode is virtually identical to that of RC-LH1 complexes in solution (Figure 2, see also SI-3, Figure S3). The absorption spectra are sensitive to pigment-pigment interactions within the complex, and therefore it may be concluded that the structure of the complexes is not significantly affected by mono-layer formation and deposition. This is confirmed by the fact that the shape of the light-induced current action spectrum is similar to the absorption spectrum of RC-LH1 complexes (Figure 2, triangles), indicating that light-induced charge separation is still fully operational, consistent with previous studies of surface-assembled RCs and chromatophores.[42,44,49] The action spectrum also shows that the RC-LH1 complexes are the source of the generated photocurrents. It is evident from the action spectrum that pigments absorbing below 550 nm show a diminished contribution to photocurrent generation. Carotenoid molecules absorb in this region and they transfer the excitation to the RC less efficiently. From the

absorption spectrum of the LB-deposited RC-LH1 monolayers (see figure 2, and SI-3, Figure S3) we determined the surface coverage in the forward as well as the reverse dipped case. Forward dipped LB films have 5.6×10^{11} protein complexes per cm^2 whereas reverse dipped film contains 5.4×10^{11} complexes per cm^2. Adsorption of RC-LH1 complexes by incubating the gold surface for one hour in the dark at 4 ºC with a solution of detergent solubilized RC-LH1 complexes (Tris buffer, pH 8) resulted in coverage of 6×10^{11} molecules per cm^2.

We measured the light-induced current response of the LB-deposited monolayers of RC-LH1 complexes on the gold electrode under various conditions. Ubiquinone-0 (Q-0) or a mixture of Q-0 and cytochrome (cyt) *c* were used as redox mediator. The magnitude of the photocurrents was influenced by the concentration of mediators, the applied potential, and the intensity of the light source. Figure 3 (black trace) shows that by omitting both mediators from the measuring solution no

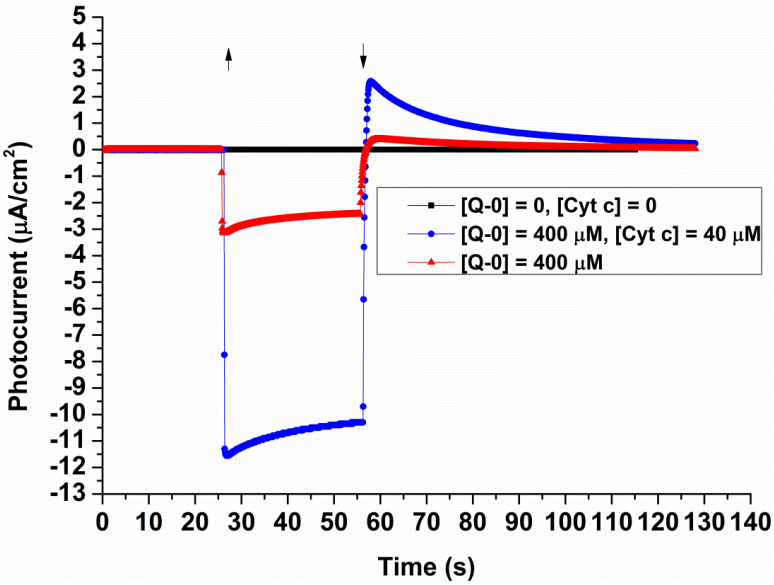

Figure 3. Photocurrents obtained from forward dipped Langmuir-Blodgett films with different redox mediator composition of the electrolyte. **Black squares**: When no redox mediators are present no current is observed. **Red triangles**: photocurrent of forward dipped LB film containing RC-LH1 using 400 µM of quinones (Q_0) as the only as redox mediator. **Blue circles**: photocurrent with both Q_0 (400 µM) and cyt *c* (40 µM). The arrows indicate when the light was switched on (upward arrow) and off (downward arrow). The applied potential is −100 mV (vs. SCE) in all cases and the light source is an 880 nm LED with 23 mW/cm² of illumination power. Tris-HCl (pH 8) is used as measuring buffer.

photocurrent is produced. The trace formed by the red triangles in Figure 3 is the response when only Q-0 is present as mediator at a potential of –100 mV (*vs.* SCE). This is well above the reduction potential of the quinone/semiquinone half reaction not only of the RC-embedded Q_A molecule , but also of the small Q-10 pool of 4-9 molecules that may be retained within the RC-LH1 complex, assuming that these values are similar for *Rhodobacter (Rb.) sphaeroides* and *Rps. acidophila.*[50] Note that the Q_A reduction potential in *Rps. acidophila* is about 100 mV more negative than in the purple bacterium *Rb. sphaeroides* since it consists of menaquinone (MK-10) rather than ubiquinone (Q-10).[51] The light-induced current response shows that electron exchange occurs between the Q-10 molecules in the RC-LH1 complexes and the Q-0 pool in solution. It is likely that electron transfer occurs directly from Q_A to Q-0 since Q-0 molecules can bind at the Q_B site of the RC, particularly at higher Q-0 concentrations, although we have to take into account that the binding constant for Q-0 is significantly lower than for Q-10, at least in the case of *Rb. sphaeroides.*[52] The current response with only Q-0 as mediator saturates, with a peak value of about 12 $\mu A/cm^2$, at a Q-0 concentration of about 3 mM (see SI-3, Fig. S4) which is comparable to that observed for the turn-over rate of Q-0 by isolated reaction centers in solution. [53]

The current response in the presence of only Q-0 (Fig. 3) shows a transient component with a relative amplitude which increases with the Q-0 concentration (see SI-3, Figure S4). This feature can be attributed to the storage and equilibration of charge in the Q-0 pool in solution. The reverse current peak that is observed when the light is switched off is consistent with this interpretation, presumably resulting from charge recombination. The amplitude of the reverse current peak also increases with increasing concentration, following the storage capacity of the solution. It is reminiscent of the alternating current response of RC-LH1 complexes from *Rb. sphaeroides* in a photoelectrochemical cell upon illumination with N,N,N',N'-tetramethyl-p-phenylenediamine as mediator, reported by Tan and co-workers.[10]

The experiments provide evidence for direct electron transfer from the gold electrode to the special pair in the RC complex at negative potentials. The results also show that Q-0 is an effective mediator for light-induced current generation by RC-LH1 complexes that are directly immobilized on a gold electrode in an electrochemical cell. Nevertheless, earlier experiments have indicated that

photocurrent generation can be enhanced by the addition of cyt *c* to the solution.[13,22] Indeed, if cyt *c* is added as an extra mediator a significant increase of the photocurrent is observed (Figure 3, blue circles).

When the conditions are optimized in terms of mediator concentrations and applied potential, we obtain the results shown in Figure 4. Here we compare the photocurrent response of the LB film in forward and reverse dipped samples with that obtained by adsorption of RC-LH1 from solution. The latter was carried out by incubating the gold electrode with a solution of isolated RC-LH1 complexes for 1 hour in the dark at 4 ºC. The electrode was then rinsed with buffer to remove unattached complexes.

The current reponse shown in Figure 4 is in stark contrast with that observed at positive potentials (see SI-3, Figure S6). In that case the photocurrent is dominated

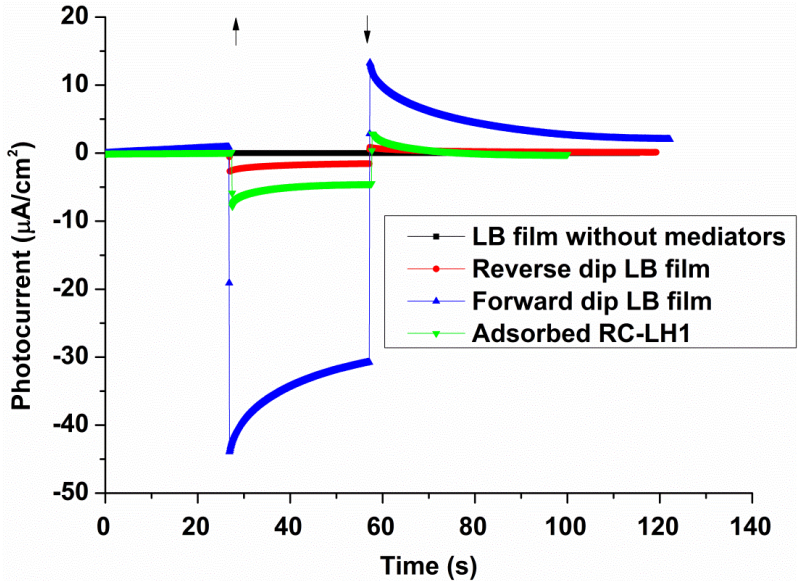

Figure 4. Photocurrent produced with different methods. Photocurrents were obtained from forward dipped LB deposition (blue triangles), reverse dipped LB film (red circles) and adsorbed (incubated for one hour on the electrode and then rinsed, green triangles) RC-LH1 complexes on gold electrode. The arrows indicate when the light is switched on (arrow pointing upwards) and when the light is switched off (arrow pointing downwards). The applied potential is −175 mV (vs. SCE) in all cases and the light source is an 880 nm LED with 23 mW/cm² of illumination power. Q-0 (1600 μM) and cyt c (320 μM) were used as charge carriers in the buffer solution.

by a fast transient response with a sign which is opposite to that of the signal in Figure 4. This can be attributed to the lower driving force for electron transfer from the electrode to the RC, and the loss of reducing capacity of the cyt *c* mediator. The fast transient response is likely due to the reduction of the quinones in the surface-assembled RCs.

At negative potentials, a major difference in photocurrent response can be observed for forward dipping compared to reverse dipping and simple incubation (*cf*. Figure 4). A maximum current density of 45 μA/cm^2 was recorded for the forward dipped case, 3 μA/cm² for the reverse dipped sample, and 8 μA/cm² for adsorbed RC-LH1. The concentration of Q-0 and cyt *c* used in all three cases was 1600 μM and 320 μM, respectively, and the applied potential was −175 mV at which the response was maximal (see SI-3, Figure S6). The light intensity at the gold surface was 23 mW/cm^2 in all three experiments, corrected for absorption by the gold layer.

The forward dipped LB film generated a peak photocurrent density of 45 μA/cm^2 under light illumination of 23 mW/cm^2 (at λ = 880 nm) using Q-0 and cyt *c* as redox mediators. This compares very favorably with results obtained previously using RC-LH1 from *Rps. acidophila*, where maximally 25 μA/cm^2 could be obtained but at twenty times higher intensity of light illumination.[13] The results presented here thus show the largest photocurrent per photosynthetic complex reported to date. Recently, Mershin and co-workers reported a photocurrent of 362 μA/cm^2 under AM1.5 solar irradiation, obtained by a photovoltaic device with photosystem 1 complexes interconnected to TiO2. This very high photocurrent could be obtained by three dimensional structuring of the electrode which enhanced the effective surface area by a factor of 200.[54] If a similar enhancement factor would apply to the case of RC-LH1 complexes we would obtain a peak current of the order of milliamperes per cm^2.

Previous reports on comparison of ET efficiency for two different orientations of RCs have shown more efficient electron transfer for RC with the electron donor side facing the electrode compared to the opposite orientation.[21,25] The large difference in photocurrent response of the forward and reverse dipped LB films suggests that we have different orientations of RC-LH1 complexes in these cases. In forward dipping we seem to have primary electron donor side close to the electrode whereas reverse dipping results in the opposite orientation. Comparison

with simple incubation supports our earlier conclusion that RC-LH1 complexes upon adsorption have a preferred orientation, with the primary donor of the RC facing the gold. The photo-current density for forward dipped LB films is much larger than that of solution-adsorbed RC-LH1 complexes though, which can be attributed to a significant fraction with unfavorable RC-LH1 orientation when adsorbed from solution, compared to the more uniformly oriented monolayers obtained by LB deposition.

Finally, the internal quantum efficiency is calculated by taking the ratio of the number of electrons generated per second to the number of photons absorbed per second. The number of electrons produced on our electrode is calculated from the maximum measured photocurrent density of 45 $\mu A/cm^2$ which is equivalent to $5.7x10^{14}$ electrons per second. The number of photons absorbed on our electrode per second is estimated from the measured absorbance of the LB film and our light illumination intensity. We measured the absorbance of our LB film monolayer to be 0.0038, which leads to $1.8x10^{15}$ photons being absorbed per second. This result in a quantum efficiency of 32 %. (see SI-3 for detailed calculations).

3.4 Conclusion

We have used the Langmuir-Blodgett technique to deposit isolated bacterial RC-LH1 complexes on a bare gold electrode and showed that this method retains the functionality of the proteins, allows the control of the orientation of the protein, and increases the photocurrent output making it a promising method for fabrication of biosensors and biosolar cells. The highest photocurrent observed was 45 μA/cm2 with an internal quantum efficiency of up to 32% under 23 mW/cm2 (at λ = 880 nm) light illumination intensity. This photocurrent is the highest of any single-layered photosynthetic protein complex to date, without any modifications to the proteins or substrate, and under ambient conditions.

References

1. Blankenship, R. E.; Tiede, D. M.; Barber, J.; Brudvig, G. W.; Fleming, G.; Ghirardi, M.; Gunner, M. R.; Junge, W.; Kramer, D. M.; Melis, A.; Moore, T. A.; Moser, C. C.; Nocera, D. G.; Nozik, A. J.; Ort, D. R.; Parson, W. W.; Prince, R. C.; Sayre, R. T. Comparing Photosynthetic and Photovoltaic Efficiencies and Recognizing the Potential for Improvement. *Science* **2011,** *332* (6031), 805-809.

2. Amao, Y.; Kuroki, A. Photosynthesis Organ Grana from Spinach Adsorbed Nanocrystalline TiO2 Electrode for Photovoltaic Conversion Device. *Electrochemistry* **2009,** *77* (10), 862-864.

3. Badura, A.; Guschin, D.; Kothe, T.; Kopczak, M. J.; Schuhmann, W.; Rogner, M. Photocurrent generation by photosystem 1 integrated in crosslinked redox hydrogels. *Energy & Environmental Science* **2011,** *4* (7), 2435-2440.

4. Ciesielski, P. N.; Hijazi, F. M.; Scott, A. M.; Faulkner, C. J.; Beard, L.; Emmett, K.; Rosenthal, S. J.; Cliffel, D.; Kane, J. G. Photosystem I - based biohybrid photoelectrochemical cells. *Bioresour. Technol.* **2010,** *101* (9), 3047-3053.

5. Das, R.; Kiley, P. J.; Segal, M.; Norville, J.; Yu, A. A.; Wang, L. Y.; Trammell, S. A.; Reddick, L. E.; Kumar, R.; Stellacci, F.; Lebedev, N.; Schnur, J.; Bruce, B. D.; Zhang, S. G.; Baldo, M. Integration of photosynthetic protein molecular complexes in solid-state electronic devices. *Nano Letters* **2004,** *4* (6), 1079-1083.

6. Frolov, L.; Rosenwaks, Y.; Carmeli, C.; Carmeli, I. Fabrication of a photoelectronic device by direct chemical binding of the photosynthetic reaction center protein to metal surfaces. *Advanced Materials* **2005,** *17* (20), 2434-+.

7. Giardi, M. T.; Pace, E. Photosynthetic proteins for technological applications. *Trends in Biotechnology* **2005,** *23* (5), 257-263.

8. Lebedev, N.; Trammell, S. A.; Tsoi, S.; Spano, A.; Kim, J. H.; Xu, J.; Twigg, M. E.; Schnur, J. M. Increasing efficiency of photoelectronic conversion by encapsulation of photosynthetic reaction center proteins in arrayed carbon nanotube electrode. *Langmuir* **2008,** *24* (16), 8871-8876.

9. Takshi, A.; Madden, J. D. W.; Mahmoudzadeh, A.; Saer, R.; Beatty, J. T. A Photovoltaic Device Using an Electrolyte Containing Photosynthetic Reaction Centers. *Energies* **2010,** *3* (11), 1721-1727.

10. Tan, S. C.; Crouch, L. I.; Jones, M. R.; Welland, M. Generation of alternating current in response to discontinuous illumination by photoelectrochemical cells based on photosynthetic proteins. *Angew. Chem. Int. Ed Engl.* **2012,** *51* (27), 6667-6671.

11. Tan, S. C.; Crouch, L. I.; Mahajan, S.; Jones, M. R.; Welland, M. E. Increasing the open-circuit voltage of photoprotein-based photoelectrochemical cells by manipulation of the vacuum potential of the electrolytes. *ACS Nano* **2012,** *6* (10), 9103-9109.

12. Yehezkeli, O.; Tel-Vered, R.; Wasserman, J.; Trifonov, A.; Michaeli, D.; Nechushtai, R.; Willner, I. Integrated photosystem II-based photo-bioelectrochemical cells. *Nat. Commun.* **2012,** *3*, 742.

13. den Hollander, M. J.; Magis, J. G.; Fuchsenberger, P.; Aartsma, T. J.; Jones, M. R.; Frese, R. N. Enhanced photocurrent generation by photosynthetic bacterial reaction centers through molecular relays, light-harvesting complexes, and direct protein-gold interactions. *Langmuir* **2011,** *27* (16), 10282-10294.

14. Kato, M.; Cardona, T.; Rutherford, A. W.; Reisner, E. Photoelectrochemical water oxidation with photosystem II integrated in a mesoporous indium-tin oxide electrode. *J. Am. Chem. Soc.* **2012,** *134* (20), 8332-8335.

15. Magis, G. J.; den Hollander, M. J.; Onderwaater, W. G.; Olsen, J. D.; Hunter, C. N.; Aartsma, T. J.; Frese, R. N. Light harvesting, energy transfer and electron cycling of a native photosynthetic membrane adsorbed onto a gold surface. *Biochim. Biophys. Acta* **2010,** *1798* (3), 637-645.

16. Mershin, A.; Matsumoto, K.; Kaiser, L.; Yu, D.; Vaughn, M.; Nazeeruddin, M. K.; Bruce, B. D.; Graetzel, M.; Zhang, S. Self-assembled photosystem-I biophotovoltaics on nanostructured TiO(2)and ZnO. *Sci. Rep.* **2012,** *2*, 234.

17. Nakamura, C.; Hasegawa, M.; Yasuda, Y.; Miyake, J. Self-assembling photosynthetic reaction centers on electrodes for current generation. *Applied Biochemistry and Biotechnology* **2000,** *84-6*, 401-408.

18. Yaghoubi, H.; Li, Z.; Jun, D.; Saer, R.; Slota, J. E.; Beerbom, M.; Schlaf, R.; Madden, J. D.; Beatty, J. T.; Takshi, A. The Role of Gold-Adsorbed Photosynthetic Reaction Centers and Redox Mediators in the Charge Transfer and Photocurrent Generation in a Bio-Photoelectrochemical Cell. *Journal of Physical Chemistry C* **2012,** *116* (47), 24868-24877.

19. Zhao, J. Q.; Liu, B. H.; Zou, Y. L.; Xu, C. H.; Kong, J. L. Photoelectric conversion of photosynthetic reaction center in multilayered films fabricated by layer-by-layer assembly. *Electrochimica Acta* **2002,** *47* (12), 2013-2017.

20. Kondo, M.; Nakamura, Y.; Fujii, K.; Nagata, M.; Suemori, Y.; Dewa, T.; Iida, K.; Gardiner, A. T.; Cogdell, R. J.; Nango, M. Self-assembled monolayer of light-harvesting core complexes from photosynthetic bacteria on a gold electrode modified with alkanethiols. *Biomacromolecules.* **2007,** *8* (8), 2457-2463.

21. Kondo, M.; Iida, K.; Dewa, T.; Tanaka, H.; Ogawa, T.; Nagashima, S.; Nagashima, K. V.; Shimada, K.; Hashimoto, H.; Gardiner, A. T.; Cogdell, R. J.; Nango, M. Photocurrent and electronic activities of oriented-His-tagged photosynthetic light-harvesting/reaction center core complexes assembled onto a gold electrode. *Biomacromolecules.* **2012,** *13* (2), 432-438.

22. Lebedev, N.; Trammell, S. A.; Spano, A.; Lukashev, E.; Griva, I.; Schnur, J. Conductive wiring of immobilized photosynthetic reaction center to electrode by cytochrome C. *J. Am. Chem. Soc.* **2006,** *128* (37), 12044-12045.

23. Manocchi, A. K.; Baker, D. R.; Pendley, S. S.; Nguyen, K.; Hurley, M. M.; Bruce, B. D.; Sumner, J. J.; Lundgren, C. A. Photocurrent generation from surface assembled photosystem I on alkanethiol modified electrodes. *Langmuir* **2013,** *29* (7), 2412-2419.

24. Reiss, B. D.; Hanson, D. K.; Firestone, M. A. Evaluation of the photosynthetic reaction center protein for potential use as a bioelectronic circuit element. *Biotechnology Progress* **2007,** *23* (4), 985-989.

25. Trammell, S. A.; Spano, A.; Price, R.; Lebedev, N. Effect of protein orientation on electron transfer between photosynthetic reaction centers and carbon electrodes. *Biosens. Bioelectron.* **2006,** *21* (7), 1023-1028.

26. Trammell, S. A.; Griva, I.; Spano, A.; Tsoi, S.; Tender, L. M.; Schnur, J.; Lebedev, N. Effects of distance and driving force on photoinduced electron transfer between photosynthetic reaction centers and gold electrodes. *Journal of Physical Chemistry C* **2007,** *111* (45), 17122-17130.

27. Ciesielski, P. N.; Scott, A. M.; Faulkner, C. J.; Berron, B. J.; Cliffel, D. E.; Jennings, G. K. Functionalized nanoporous gold leaf electrode films for the immobilization of photosystem I. *ACS Nano* **2008,** *2* (12), 2465-2472.

28. Faulkner, C. J.; Lees, S.; Ciesielski, P. N.; Cliffel, D. E.; Jennings, G. K. Rapid assembly of photosystem I monolayers on gold electrodes. *Langmuir* **2008,** *24* (16), 8409-8412.

29. Gunther, D.; LeBlanc, G.; Prasai, D.; Zhang, J. R.; Cliffel, D. E.; Bolotin, K. I.; Jennings, G. K. Photosystem I on graphene as a highly transparent, photoactive electrode. *Langmuir* **2013,** *29* (13), 4177-4180.

30. Lu, Y.; Xu, J.; Liu, Y.; Liu, B.; Xu, C.; Zhao, D.; Kong, J. Manipulated photocurrent generation from pigment-exchanged photosynthetic proteins adsorbed to nanostructured WO3-TiO2 electrodes. *Chem. Commun. (Camb.)* **2006,** (7), 785-787.

31. Lu, Y. D.; Liu, Y.; Xu, J. J.; Xu, C. H.; Liu, B. H.; Kong, J. L. Bio-nanocomposite photoelectrode composed of the bacteria photosynthetic reaction center entrapped on a nanocrystalline TiO2 matrix. *Sensors* **2005,** *5* (4-5), 258-265.

32. Lukashev, E. P.; Nadtochenko, V. A.; Permenova, E. P.; Sarkisov, O. M.; Rubin, A. B. Electron phototransfer between photosynthetic reaction centers of the bacteria Rhodobacter sphaeroides and semiconductor mesoporous TiO2 films. *Doklady Biochemistry and Biophysics* **2007,** *415* (1), 211-216.

33. Mahmoudzadeh, A.; Saer, R.; Jun, D.; Mirvakili, S. M.; Takshi, A.; Iranpour, B.; Ouellet, E.; Lagally, E. T.; Madden, J. D. W.; Beatty, J. T. Photocurrent generation by direct electron transfer using photosynthetic reaction centres. *Smart Materials & Structures* **2011,** *20* (9).

34. Matsumoto, K.; Nomura, K.; Tohnai, Y.; Fujioka, S.; Wada, M.; Erabi, T. Immobilization of photosynthetic reaction center complexes onto a hydroquinonethiol-modified gold electrode. *Bulletin of the Chemical Society of Japan* **1999,** *72* (10), 2169-2175.

35. Nikandrov, V. V.; Borisova, Y. V.; Bocharov, E. A.; Usachev, M. A.; Nizova, G. V.; Nadtochenko, V. A.; Lukashev, E. P.; Trubitsin, B. V.; Tikhonov, A. N.; Kurashov, V. N.; Mamedov, M. D.; Semenov, A. Y. Photochemical properties of photosystem 1 immobilized in a mesoporous semiconductor matrix. *High Energy Chemistry* **2012,** *46* (3), 200-205.

36. Terasaki, N.; Iwai, M.; Yamamoto, N.; Hiraga, T.; Yamada, S.; Inoue, Y. Photocurrent generation properties of Histag-photosystem II immobilized on nanostructured gold electrode. *Thin Solid Films* **2008,** *516* (9), 2553-2557.

37. Atkins, K. J.; Honeybourne, C. L. Langmuir-Blodgett-Films of New Amphiphilic Electrooptically Active Charge-Transfer Dyes. *Journal of Physics-Condensed Matter* **1991,** *3*, S319-S327.

38. Bernard, J.; Talon, H.; Orrit, M.; Mobius, D.; Personov, R. I. Stark-Effect in Hole-Burning Spectra of Dye-Doped Langmuir-Blodgett-Films. *Thin Solid Films* **1992,** *217* (1-2), 178-186.

39. Byrd, H.; Pike, J. K.; Talham, D. R. Inorganic Monolayers Formed at An Organic Template - A Langmuir-Blodgett Route to Monolayer and Multilayer Films of Zirconium Octadecylphosphonate. *Chemistry of Materials* **1993,** *5* (5), 709-715.

40. Chakraborty, S.; Bhattacharjee, D.; Hussain, S. A. Formation of nanoscale aggregates of a coumarin derivative in Langmuir-Blodgett film. *Applied Physics A-Materials Science & Processing* **2013,** *111* (4), 1037-1043.

41. Choi, J. W.; Nam, Y. S.; Kong, B. S.; Lee, W. H.; Park, K. M.; Fujihira, M. Bioelectronic device consisting of cytochrome c/poly-L-aspartic acid adsorbed hetero-Langmuir-Blodgett films. *Journal of Biotechnology* **2002,** *94* (3), 225-233.

42. Facci, P.; Erokhin, V.; Paddeu, S.; Nicolini, C. Surface pressure induced structural effects in photosynthetic reaction center Langmuir-Blodgett films. *Langmuir* **1998,** *14* (1), 193-198.

43. Fukuda, K.; Shibasaki, Y.; Nakahara, H.; Tagaki, W.; Takahashi, H.; Tamura, S.; Kawabata, Y. Photopolymerization of A Omega-Tricosenoyl Derivative of Beta-Cyclodextrin in Langmuir-Blodgett-Films. *Thin Solid Films* **1992,** *210* (1-2), 387-389.

44. Yasuda, Y.; Hirata, Y.; Sugino, H.; Kumei, M.; Hara, M.; Miyake, J.; Fujihira, M. Langmuir-Blodgett-Films of Reaction Centers of Rhodopseudomonas-Viridis - Photoelectric Characteristics. *Thin Solid Films* **1992,** *210* (1-2), 733-735.

45. Yoshida, J.; Saruwatari, K.; Kameda, J.; Sato, H.; Yamagishi, A.; Sun, L. S.; Corriea, M.; Villemure, G. Electron transfer through clay monolayer films fabricated by the Langmuir- Blodgett technique. *Langmuir* **2006,** *22* (23), 9591-9597.

46. Zarbakhsh, A.; Campana, M.; Mills, D.; Webster, J. R. Structural studies of aliphatic substituted phthalocyanine-lipid multilayers. *Langmuir* **2010,** *26* (19), 15383-15387.

47. Zasadzinski, J. A.; Viswanathan, R.; Madsen, L.; Garnaes, J.; Schwartz, D. K. Langmuir-Blodgett-Films. *Science* **1994,** *263* (5154), 1726-1733.

48. Zaitsev, S. Y.; Kalabina, N. A.; Zubov, V. P.; Lukashev, E. P.; Kononenko, A. A.; Uphaus, R. A. Monolayers of Photosynthetic Reaction Centers of Green and Purple Bacteria. *Thin Solid Films* **1992,** *210* (1-2), 723-725.

49. Alegria, G.; Dutton, P. L. Langmuir-Blodgett Monolayer Films of Bacterial Photosynthetic Membranes and Isolated Reaction Centers - Preparation, Spectrophotometric and Electrochemical Characterization .1. *Biochimica et Biophysica Acta* **1991,** *1057* (2), 239-257.

50. Comayras, F.; Jungas, C.; Lavergne, J. Functional consequences of the organization of the photosynthetic apparatus in Rhodobacter sphaeroides. I. Quinone domains and excitation transfer in chromatophores and reaction center.antenna complexes. *J. Biol. Chem.* **2005,** *280* (12), 11203-11213.

51. Hiraishi, A.; Hoshino, Y.; Kitamura, H. Isoprenoid Quinone Composition in the Classification of Rhodospirillaceae. *Journal of General and Applied Microbiology* **1984,** *30* (3), 197-210.

52. Diner, B. A.; Schenck, C. C.; Devitry, C. Effect of Inhibitors, Redox State and Isoprenoid Chain-Length on the Affinity of Ubiquinone for the Secondary Acceptor Binding-Site in the Reaction Centers of Photosynthetic Bacteria. *Biochimica et Biophysica Acta* **1984,** *766* (1), 9-20.

53. Gerencser, L.; Maroti, P. Turnover of ubiquinone-0 at the acceptor side of photosynthetic reaction center. *European Biophysics Journal with Biophysics Letters* **2008,** *37* (7), 1195-1205.

54. Mershin, A.; Matsumoto, K.; Kaiser, L.; Yu, D.; Vaughn, M.; Nazeeruddin, M. K.; Bruce, B. D.; Graetzel, M.; Zhang, S. Self-assembled photosystem-I biophotovoltaics on nanostructured TiO(2)and ZnO. *Sci. Rep.* **2012,** *2*, 234.

SI-3

Chapter 3: Supporting Information

SI-3.1 Materials and Methods

RC-LH1 Isolation

RC-LH1 complexes from *Rps. acidophila* were isolated by using the protocol from Law et al. (1999) and suspended in buffer with 10 mM Tris (pH 8), supplemented with 0.1% Lauryldimethylamine-N-oxide(LDAO) and 1 mM EDTA(Law et al. 1999)

Gold Working Electrodes:

The working electrodes were prepared by sputtering gold on clean glass cover slips (Van Baarle et al.2003). The glass cover slips (25 mm diameter, 0.13-0.16 mm thickness) were purchased from Menzel-Gläser and cleaned prior to sputtering using various steps. First, the cover slips were sonicated for one hour in methanol, washed with milli-Q water, and dried under the nitrogen flow. The glass cover slips were then ozone-cleaned by using a UVP PR-100, UV-ozone Photoreactor, for one hour. Gold was deposited on the clean glass cover slips by using a magnetron sputtering system (ATC 1800-F, AJA Corporation). A thin layer (1-2 nm thick) of molybdenum-germanium (MoGe) was deposited first in order to serve as an

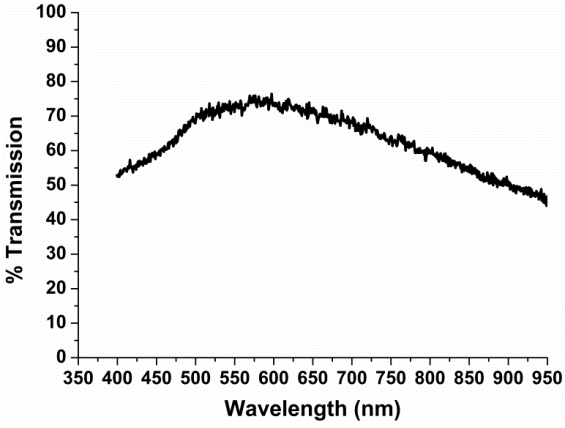

Figure S1.
Optical transmission spectrum of a 12 nm thick gold layer deposited on a microscope glass cover slip. The spectrum was measured with a fiber-coupled spectrometer (QE6500, Ocean Optics Inc., USA).

adhesion layer between the gold and the glass surface. A homogeneous, 12 nm thick layer of gold was then sputtered on top of it. MoGe was sputtered at the rate of 1.32 nm/min in a 10 mTorr argon environment, whereas for the gold the sputtering rate was 9.06 nm/min in an argon atmosphere mixed with 1% and oxygen at a total pressure of 10 mTorr. Gold coated glass cover slips were then stored in a desiccator (at most for a few days) until they were used. This gold deposition protocol results in very flat, homogenous gold layers with a root-mean-square roughness of 2-3 Å and a uniform thickness across the full surface of the cover slip. These properties were very reproducible, and are directly associated with the presence of the MoGe wetting layer. Figure S1 shows the transmission spectrum of such a cover slip when coated with a gold layer of 12 nm thick.

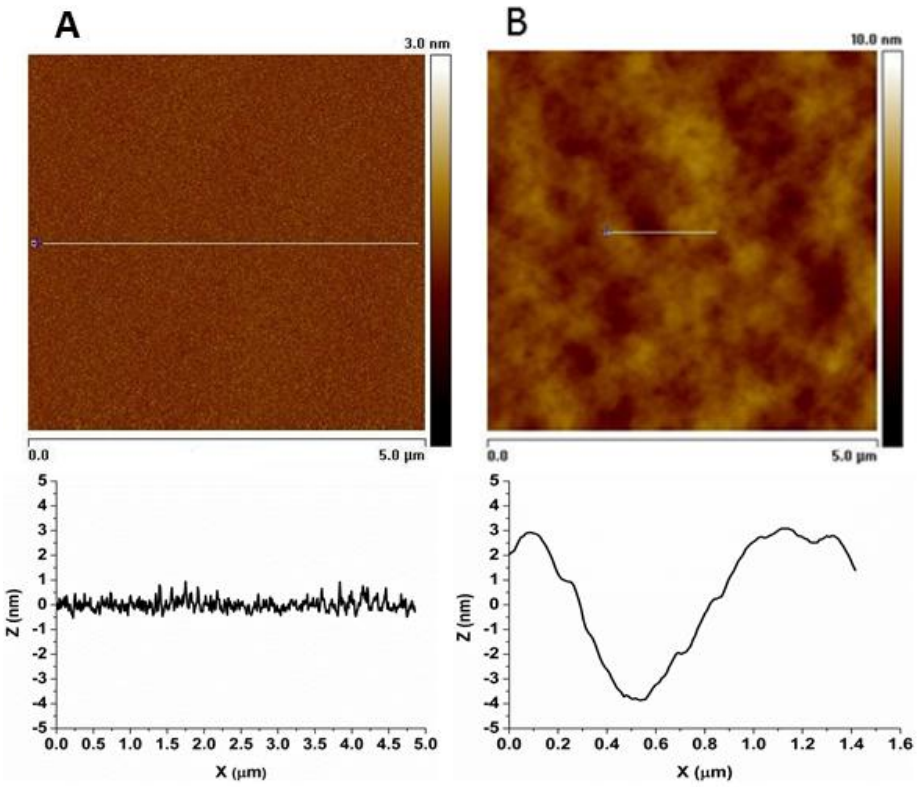

Figure S2. *Top*: Tapping mode AFM image of freshly sputtered gold electrode (left) and Langmuir Blodgett film (right) deposited on gold electrode, imaging was performed under ambient conditions. *Bottom:* Height profiles of the AFM images along the lines in the corresponding top pnales.

Langmuir Blodgett Deposition

A KSV Nima trough (KSV instruments Co., Helsinki, Finland) was used to deposit Langmuir-Blodgett films of isolated RC-LH1 complexes on the gold electrodes. The sub-phase of the LB trough initially contained only milli-Q water. A solution of isolated RC-LH1 complexes (1 mg/ml concentration) was then spread over the water surface and the air-water interface was allowed to settle for 15 minutes. After subsequently compressing the surface layer to a surface pressure of 50 mN/m, the gold coated glass cover slip was vertically dipped into the trough at a velocity of 1 mm/min while maintaining a constant surface pressure of 50 mN/m during the LB deposition. After dipping the slide completely into the water sub-phase, the slide was pulled out at the highest available speed to avoid any deposition during the extraction. For reverse dipping, the gold coated glass cover slip was first dipped into the sub-phase before spreading the RC-LH1 solution on the surface of the milliQ water. After 15 min the slide was vertically extracted with a velocity of 1 mm/min while keeping the surface pressure constant at 50 mN/m.

Atomic Force Microscopy

The topography of the Langmuir-Blodgett film of RC-LH1 complexes on the gold electrode was observed by imaging in tapping mode and in air using a commercial atomic force microscope, equiped with an E-Scanner (AFM, Nanoscope IIIa, Veeco, USA). A typical image is shown in Figure S2. Standard Si-nitride probes with a resonance frequency of 75 kHz and a spring constant of 2.8 Nm^{-1} were used for imaging. Topography of the freshly sputtered bare gold electrode (S2 A) and gold electrode after Langmuir-Blodgett film deposition (S2 B) is shown in figure S2.

Surface coverage of RC-LH1 on gold electrode by absorption spectra

The surface coverage of RC-LH1 was calculated from the absorption spectra of Langmuir Blodgett films deposited in forward dip, reverse dip, and of adsorbed RC-LH1 complexes from the solution. The absorption spectra were recorded by using a fiber-coupled spectrometer (QE 6500, Ocean Optics Inc.), equipped with a halogen light source. The spectra are shown in Figure S3. The spectra were corrected for reflection and absorption by the gold layer by using a bare gold-coated cover slip from the same coating run as a reference.

The absorption spectra were utilized to calculate the surface coverage. The measured absorbance for the forward dipped LB film at 885 nm was 0.00375 (this is half of the measured absorbance of 0.0075 because we have LB film on both sides of the slide) the numbers of RC-LH1 complexes per cm^2 for forward dipped LB film are calculated to be 5.6×10^{11}, for reverse dipping the number of complexes is 5.4×10^{11}, whereas the sample with adsorbed RC-LH1 has 6×10^{11} molecules per cm^2

Photocurrent Measurement

Light induced current measurements were carried out using a potentiostat (Autolab PGSTAT 128N) in the conventional 3 three-electrode setup, with the gold coated glass cover slip acting as the working electrode, a standard calomel electrode as the reference, and a platinum wire serving as the counter electrode. The reference electrode and the counter electrode were inserted from the top into a home built

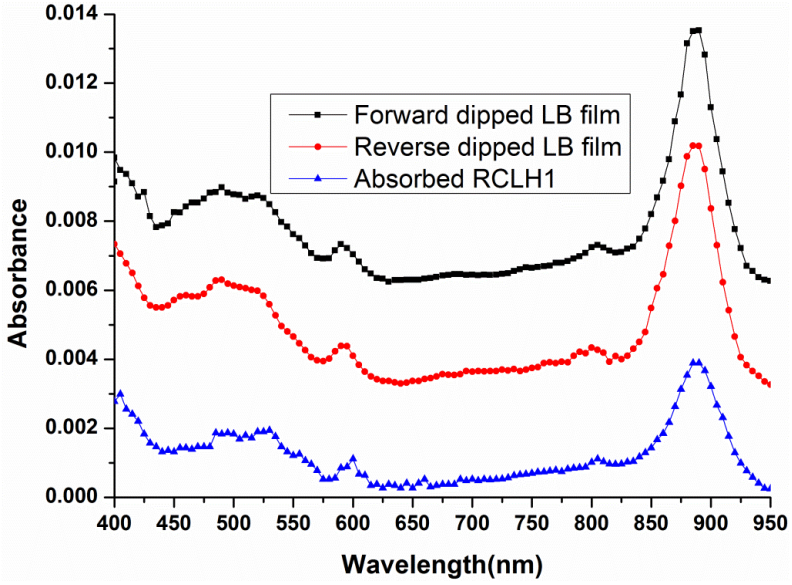

Figure S3: Absorption spectra of Langmuir Blodgett (LB) films of RC-LH1 complexes (red dots: reverse dipped, black dots: forward dipped), and of adsorbed RC-LH1 complexes (blue triangles) on gold electrodes. The sample with adsorbed RC-LH1 complexes was prepared by incubating the gold-coated glass slide with a solution of isolated RC-LH1 complexes (1 mg/ml) for one hour at 4ºC and rinsing it afterward with buffer solution (Tris HCl, pH 8). The absorption spectra if the LB-films are vertically displaced by steps of 0.003 absorbance units for better viewing.

electrochemical cell. The gold coated glass cover slip was incorporated as the base of the cell and functioned as the working electrode with an active diameter of 16 mm. A high power light emitting diode (LED) purchased from Roithner LaserTechnik was used as our light source. This LED (LED880-66-60) has a central wavelength of 880 nm and a 50 nm bandwidth (FWHM). The LED was operated with 800 mA at 7.6 V, resulting in a light intensity of 23 mW/cm^2 at the surface of the gold electrode in the electrochemical cell, corrected for transmission of the gold layer. In the case of the action spectra, the illumination was provided by passing white light from a halogen/tungsten lamp through a scanning monochromator with a bandwidth of 40 nm. In this case, the power of the light source reaching the cell was 2 mW/cm^2 at 880 nm.

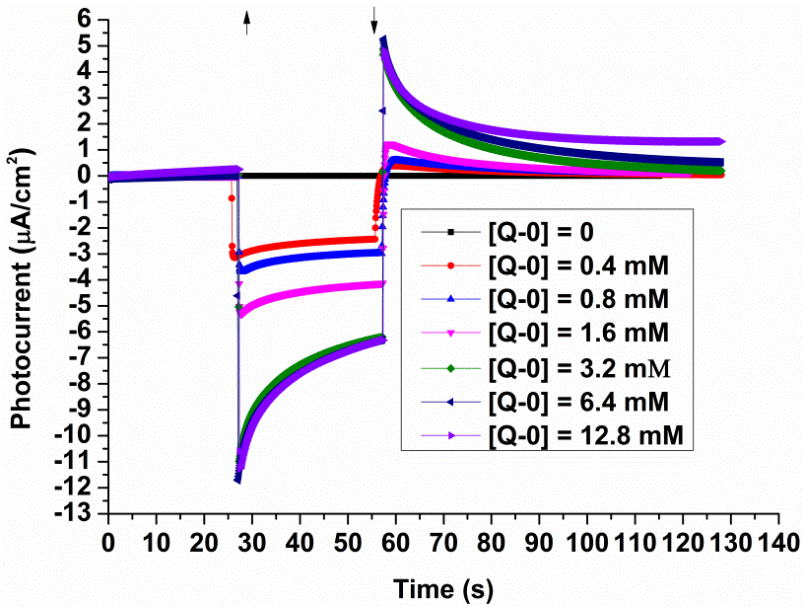

Figure S4: Photocurrent generated by an LB film of RC-LH1 complexes as a function of quinone (Q-0) concentration. The photocurrent was measured with a three-electrode electrochemical cell equipped with a potentiostat and a light source. The cell was iluminated from below with an intensity of 23 mW/cm^2 at 880 nm (bandwidth 50 nm). The upward arrow (↑) in the figure indicates the moment that the light was turned on whereas the downward arrow (↓) is the moment that the light was turned off. The magnitude of photocurrent increased with increasing the concentration of Q-0. The highest peak-current of 12 μA/cm^2 was reached at 3.2 mM of Q-0 as mediator; no further increase was observed at higher concentrations.

A computer controlled shutter was placed between the light source and the measuring cell to switch the light illumination on/off. The redox mediators used in the measuring solution were cytochrome *c* from equine heart and 2,3-dimethoxy-5-methyl-*p*-benzoquinone (ubiquinone-0, Q-0), both purchased from Sigma. The photocurrent response with only Q-0 as mediator is shown in Figure S4 as a function of mediator concentration.

At positive potentials the photocurrent response is very different, as shown in Figure S5. The light-induced current is dominated by a fast transient response when the light is switched on. This likely due to the reduction of the quinones contained in the RCs which will be re-oxidized via the Q-0 pool in solution and the working electrode.

Variation of Photocurrent with applied Potential

The light-induced current response of the RC-LH1 monolayer/gold electrode was measured as a function of applied potential. The highest photocurrent was

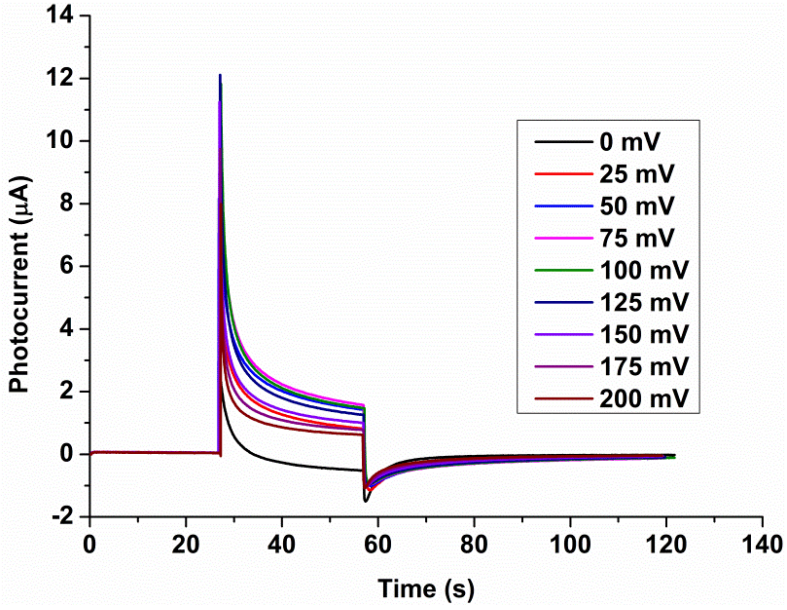

Figure S5: Photocurrent from a forward dipped LB film of RC-LH1 complexes deposited on a bare gold surface at different positive applied potentials in the presence of Q-0 (1600 μM) and cyt *c* (320 μM) as mediators. Applied potentials ranged from between 0 to 200 mV in steps of 25 mV (vs SCE). The upward (↑) and downward arrow (↓) indicate the moment that light illumination was turned on and off, respectively.

recorded at -175 mV for a forward dipped LB-deposited RC-LH1 layer, see figure S6.

Quantum Efficiency (QE) calculations

The quantum efficiency is estimated by taking the ratio of the number of electrons produced per second (N_e) to the number of absorbed photons per second (N_{ap}) (Ciesielski et al. 2010).

$$Q_E = N_e/N_{ap}$$

In order to determine how many photons are absorbed, we need to know the photon flux of the light source which consists of a light-emitting diode (LED), centered at λ = 880 nm with a power density of 23 mW/cm^2 at the sample (corrected for transmission of the gold layer). Taking into account the effective area of 2.01 cm^2 of the working electrode we obtain for the incident number of photons per second at the sample:

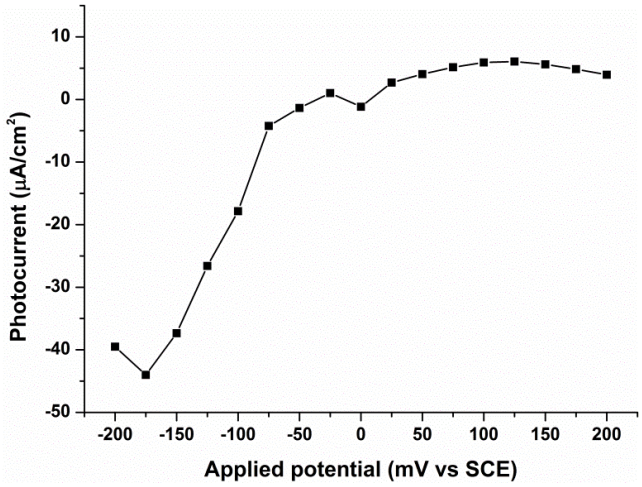

Figure S6: Variation of the peak values of the photocurrent from a LB-deposited RC-LH1 layer (forward dipped) with applied potential. The photocurrent was measured in an electrochemical cell equipped with a potentiostat. The layer was deposited on the working electrode which was incorporated into the measuring cell filled with buffer solution (Tris HCl, pH 8) containing Q-0 (1600 µM) and cytochrome *c* (320 µM) as redox mediators. The intensity of light illumination is 23 mW/cm^2. The photocurrent was recorded at different potentials in steps of 25mV

$\phi_e = 2.05 \times 10^{17}$ photons/s

The number of photons that are actually being absorbed are given by

$$N_{ap} = \phi_e \times (1 - T),$$

where T is the transmittance. From the measured absorbance, $A = 0.00375$, we calculate that $T = 0.9914$, and thus we have

$N_{ap} = 1.76 \times 10^{15}$ photons/s

The peak photocurrent was 45 μA/cm^2 which corresponds to

$N_e = 5.647 \times 10^{14}$ electrons/s,

Adjusting this value for the effective area of the working electrode, and substituting the numbers in the equation for Q_E, we obtain $Q_E = 32$ %

References

1. Law, C.J. **1999**. PhD thesis, University of Glasgow, United Kingdom.
2. Van Baarle, G. J. C., Troianovski, A. M., Nishizaki, T., Kes, P. H. and Aarts, J. *Appl. Phys.Lett.* **2003, 82**, 1081
3. Ciesielski, P.N., Faulkner, C. J., Irwin, M. T., Gregory, J. M., Tolk, N. H., Cliffel, D. E. and Jennings, G. K. **2010.** *Adv. Funct.Mater.* **20**, 4048